

Adsorption of methyl orange from aqueous solutions using olive pomace: Akinetic and isotherm study

Wafa S Beaj^{1*}, Abdounasser Albasher Omar¹, Nawal Abdurazq Ahmad¹, Hajir Almahdi Alhinsheeri², Safa Mohammed Abdalnabi², Maram Fathi Sheemah²

¹Chemistry Department, Gharyan's Faculty of Science, Gharyan University, Gharyan, Libya.

²Undergraduate student, Chemistry Department, Gharyan's Faculty of Science, Gharyan University, Gharyan, Libya.

*Correspondence: wafa.baej83@gmail.com

Abstract:

This study investigated the potential use of olive pomace (OP) as an adsorbent to reduce the concentration of methyl orange (MO) in aqueous solutions. The effect of some important parameters on the process of adsorption was examined, including pH, adsorbent weight, temperature, contact time, agitation speed, and the initial concentration of MO. The results showed that the optimum concentration of MO was 10 ppm and the optimum pH = 2, indicating that the process of MO adsorption on the surface of the OP was better in acidic medium. The equilibrium time was 80 min at a speed of 100 rpm. The results of the study showed the significant role of OP weight, agitation speed, temperature and the contact time in increasing the adsorption efficiency. On comparing the pseudo first order and pseudo second order models, the results showed that the pseudo second order model fitted the experimental data well. The study also included testing of Langmuir and Freundlich models on the adsorption isotherm data, and it was found that experimental data obey the Freundlich isotherm. To sum up, the study showed that OP has high adsorption efficiency to remove MO by applying a simple, inexpensive method.

Keywords: Methyl orange, olive pomace, isotherms, kinetics, adsorption.

Introduction

Despite that dyes pose great environmental hazards, there is a global increase in their production through textile, cosmetics, pharmaceuticals and food industries [1, 2]. These hazards arise from the fact that most dyes have a complex aromatic structure, making them stable to light, heat and oxidizing agents, and thus difficult to degrade when exist in aquatic systems [3].

Removal of chemical contaminants from water can be achieved by a variety of methods including flocculation and coagulation, membrane separation [4,5], biological treatment [6, 7], ultra and nano filtration, photo oxidation, chemical oxidation [8, 9]. The method of choice is determined by the type of contaminant to be removed.

Many treatment methods have been developed to remove dyes from water, which include physical, chemical and biological methods. Recently, adsorption has become the most popular technique for removal of dyes due to its effectiveness, operational simplicity, low cost, and low energy requirements [10, 11]. The adsorption by agricultural waste materials seems to be feasible for dye remediation, because these materials are economic and eco-friendly due to their unique chemical composition, availability, renewability, low cost and more efficiency [12].

Azo-dyes are organic dyes that contain nitrogen as the azo group $-N=N-$ in their structures [13]. These dyes account for at least 50% of all dyes and are frequently attributed with being toxic and possibly carcinogenic [14]. Of those azo dyes, methyl orange (MO) is a carcinogenic water-soluble dye which is widely used in textile



industries, manufacturing printing paper, and research laboratories [15]. It is a stable dye that shows low biodegradability, and it is difficult to remove from aqueous solutions by common treatment methods [16]. In the past few years, many waste materials or by-products have been used as adsorbents for removing MO from water; for instance: chitosan biomass [17, 18], egg shell [19]. The use of polymeric materials [7] and clay materials such as montmorillonite [20], zeolite [21], bentonite [22] and kaolinite [15, 23], have also been reported. Many studies have reported using agricultural products to remove MO from aqueous solutions, these include: wheat bran [12], tree bark powder [24], sugar cane dust [25] and coffee grounds [10]. In a previous study, olive pomace (OP) has been used for MO removal from aqueous solutions [26]. However, the aforementioned study has not investigated the effect of some conditions, such as pH and temperature, which may affect the removal of MO from aqueous solutions by OP. Also, in that previous study kinetics have not been conducted and isotherm studies have been limited.

Therefore, the aim of the current study was to investigate the applicability of OP as an adsorbent material for removal of MO from aqueous solutions. The effect of contact time, initial dye concentration, temperature, pH, agitation speed and adsorbent dosage on the adsorption of MO onto the OP were examined. Kinetic and isotherm models were also applied to the experimental data to examine the extent of fit.

Material and Methods

Chemicals: Toluene and ethanol were of GPR grade, while sodium hydroxide (NaOH), hydrochloric acid (HCl) and MO were of analytical grade. The source of all chemicals is BDH (BDH Chemicals, Poole, UK).

A stock solution of MO (100 ppm) was prepared by dissolving 0.1 g of solid MO in sufficient double distilled water transferred to a 1L volumetric flask which was filled to the mark with double distilled water. This solution was used to prepare the other required MO solutions.

Sampling and preparation of OP for the adsorption process: About 250 g of olive OP was collected into a clean plastic bag from an olive oil mill located in Gharyan, Libya, then transferred to the lab where it was treated as follows. Firstly, the OP was immersed into 750 mL of double distilled water for 24 h, then filtered and air dried. Secondly, the remained OP was washed with 1 L of hot double distilled water, then dried at 105 °C for 2 h. The obtained OP was divided into three parts and each part was transferred to a 500 mL beaker. To each beaker 200 mL of toluene was added, and the mixture was shaken for 10 min. After that the OP was filtered and air dried. Finally, the OP was subjected to solvent extraction by soxhlet apparatus with 2.5 mL of ethanol per 1 g of OP, then the OP was dried, washed with double distilled water and dried at 105 °C for 2 h. The net weight of OP was 188 g which was stored in a glass beaker sealed with parafilm.

Factors affecting adsorption: Batch experiments were carried out to investigate the effect of six factors on the adsorption of MO onto OP, and this was accomplished by varying only one factor each time. The investigated factors were pH, contact time, temperature, OP weight, MO concentration and agitation speed. And for each factor, all the experiments were performed simultaneously. Except for the effect of the pH, adsorption experiments were carried out in the same optimum pH, which was determined before studying any other factor. HCl and NaOH (1 M) solutions were used to adjust the pH of the solution. 25 mL of MO solution was used in all the

adsorption experiments to study the effect of all factors, except in the case of contact time in which the volume was 50 mL. After completing each experiment, the remained concentration of MO and its percentage removal were determined. The condition values at which each factor investigated are shown in Table 1.

Table 1. The conditions used to investigate each factor

Condition values Factors	pH	Contact time (min)	OP weight (g)	MO Conc. (ppm)	Temp . (°C)	Agitation speed (rpm)
Ph	2-8	60	1	5	20	-
Contact time	2	30-240	1	10	20	-
OP weight	2	60	0.5-3	5	20	-
MO Conc.	2	60	1	2.5-20	20	-
Temperature	2	30	1	10	10-60	-
Agitation speed	2	30	1	10	20	0-250

Determination of percentage removal of MO: After each adsorption experiment, the absorbance of the remained MO was measured with the visible spectrophotometer (Jenway 6300 spectrophotometer, Staffordshire, UK) at 464 nm. To determine the concentration of the remained MO, a calibration curve was set using solutions of MO with a concentration of 1, 5, 10, 15, 20 ppm. After determination of the remained MO concentrations, the removal percentage of MO was calculated by equation (1)

$$\text{Removal percentage} = 100 (C_i - C_{\text{rem}}) / C_i \quad (1)$$

Where C_i represents the initial MO concentration and C_{rem} represents the remained MO concentration after each adsorption experiment.

Kinetic Studies: In order to study the kinetics of MO adsorption onto OP, six mixtures were prepared and treated as follows: 25 mL of MO (25 ppm) was added to 1 g of OP into a 100 mL conical flask, then the pH was adjusted to 2 by adding drops of either NaOH or HCl solutions. Each mixture was shaken at 100 rpm at 35° C in an orbital shaker. After 10, 20, 40, 60, 70, 80 min, aliquots of 5 ml from one individual mixture was analyzed for the remained MO.

The adsorption capacity of at any time, q_t , (mg/g) was calculated using the equation (2), while the equilibrium adsorption capacity, q_e (mg/g), was calculated using the equation (3)

$$q_t = V(C_0 - C_t) / m \quad (2)$$

$$q_e = V(C_0 - C_e) / m \quad (3)$$

Where C_0 represents the initial MO concentration, C_t represents the remained MO concentration after t time, C_e represents the remained MO concentration after equilibrium time, V represents MO solution volume (L), m represents OP weight (g). The obtained data were used to investigate the adsorption kinetics. This was achieved by applying two adsorption kinetic models, namely are pseudo-first order [27] expressed in equation (4) and pseudo second order [28] expressed in equation (5).



$$\log(q_e - q_t) = \log q_e - \frac{K_1 t}{2.303} \quad (4)$$

Where q_t and q_e are the adsorption capacities at time t and at equilibrium; respectively (mg/g), t is the contact time (min), k_1 is the rate constant of pseudo-first-order adsorption (1/min). By plotting $\log(q_e - q_t)$ versus (t) a linear relationship would be obtained if the model fits the experimental data, and the constants k_1 and calculated q_e could be determined from the slope and intercept of the plot, respectively.

$$\frac{t}{q_t} = \frac{1}{K_2 q_e^2} + \frac{t}{q_e} \quad (5)$$

q_t is the adsorption capacities at time t (mg/g), t is the contact time (min), k_2 is the rate constant of pseudo-second-order adsorption (g/(mg min)).

By plotting t/q_t versus t a linear relationship would be obtained if the model fits the experimental data. The constants q_e and k_2 could be determined from the slope and intercept of the plot, respectively.

Isotherm studies: In the adsorption process, equilibrium is established when the concentration of the adsorbate in solution is in balance with the interface concentration [29]. The equilibrium adsorption isotherms, which are mathematical equations that describe the experimental adsorption data, could be applied to obtain information such as surface properties and the adsorbent interactions [30]. To investigate the adsorption isotherm. Seven solutions of MO were prepared with concentrations of 10, 15, 20, 25, 30, 40, and 50 ppm and then treated as follows: 25 mL of each solution was added to 1 g of OP in a 100-mL conical flask, then the pH was adjusted to 2. Each mixture was shaken at 100 rpm at 30C in an orbital shaker. After 100 min each mixture was analyzed for the remained MO which represents its concentration at equilibrium.

Two equilibrium isotherms were studied: the Langmuir and the Freundlich isotherm[31], which are expressed in equation (6) and (7); respectively.

$$\frac{C_e}{q_e} = \frac{1}{Q_m k_a} + \frac{1}{Q_m} C_e \quad (6)$$

Q_m (mg/g) and K_a (L/mg) are Langmuir constants related to maximum adsorption capacity and energy of adsorption, respectively. Q_m and K_a values can be calculated from the plot between C_e/q_e versus C_e . C_e (ppm) and q_e (mg/g) are the equilibrium concentration, and the amount of dye adsorbed at equilibrium; respectively.

$$\log q_e = \log K_f + \frac{1}{n} \log C_e \quad (7)$$

K_f (mg/g(L/g)^{1/n}) and n are Freundlich constants, which are indicators of adsorption capacity and adsorption intensity, respectively. These two constants can be calculated from the plot of $\log(q_e)$ versus $\log(C_e)$. C_e is the equilibrium concentration, and q_e is the amount of dye adsorbed at equilibrium. The parameter $1/n$ is in the range between 0 and 1 that measures the adsorption intensity or surface heterogeneity. The value of the constant n can give indications of the adsorption nature as follows:

If $n = 1$ then that the partition between the two phases was independent of the concentration. If the $1/n$ value is below one, it indicates normal adsorption. On the other hand, $1/n$ being above one that indicates cooperative adsorption [32].

RESULTS AND DISCUSSION

Calibration curve: Figure 1 shows the calibration curve of MO standard solutions which was used to obtain the remained MO concentration in each adsorption experiment. The regression equation is expressed in equation (8). The coefficient of determination (R^2) of this equation was 0.997, which indicates high linearity, Thus it was statistically acceptable to use this equation for calculating the remaining of MO concentration.

$$A=0.05428 C+0.00759 \quad (8)$$

Where A is the absorbance of each MO solution, and C is MO concentration in ppm.

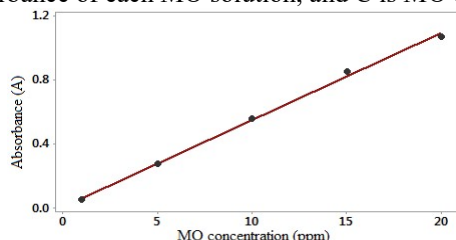


Figure (1) The calibration curve of MO standard solutions

Factors affecting adsorption:

Effect of pH: Figure (2) shows that MO adsorption on the OP was affected by pH; the higher the pH of solution, the lower the adsorbed quantity of MO. The highest percentage (56%) of adsorbed MO onto OP was in a strong acidic medium where the pH was equal to 2 (due to the presence of proton of hydrochloric acid), while the lowest percentage was 9% in a weak basic medium (pH=8). The reason for this decrease is that hydroxyl ions (from NaOH solution) compete with methyl orange on adsorption at the active sites because they have the same charge [33, 34].

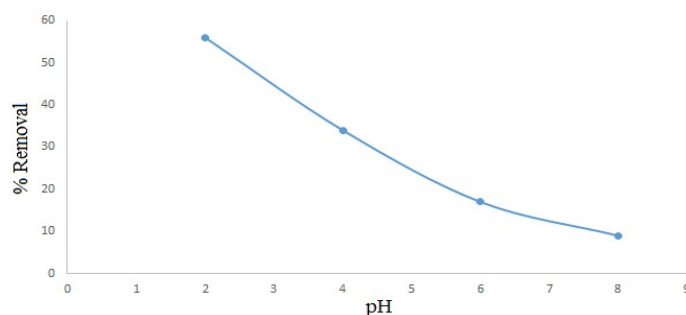


Figure (2) Increasing of MO removal percentage as pH decreased

Effect of adsorbent weight: It was observed that the removal percentage of MO increased with increasing the weight of the adsorbent (OP) as shown in Figure (3). The highest percentage of adsorption (91%) was achieved using 3 g of OP. As the OP weight increased, the number of active sites and the OP surface area increased, this led to increase in adsorption quantity [35].

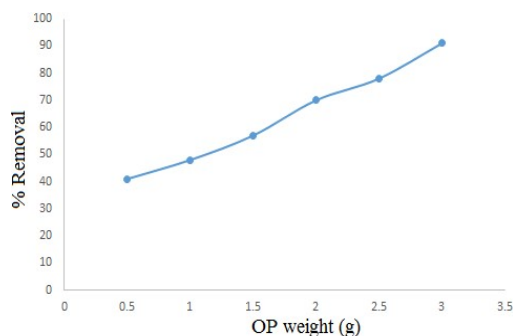


Figure (3) Increasing of MO removal percentage as the weight of OP increased

Effect of contact time: Fig (4) shows that increasing the contact time between MO and OP increased the removal percentage. It was shown that the lowest percentage of MO adsorption was 24% after 30 min. After 60 min, the adsorption rate increased and the removal percentage nearly doubled and reached 44%. The highest removal percentage of MO adsorption was at 240 min, which was 79%. This increase in adsorption could be explained by the presence of sufficient active sites on OP surface as the contact time increased.

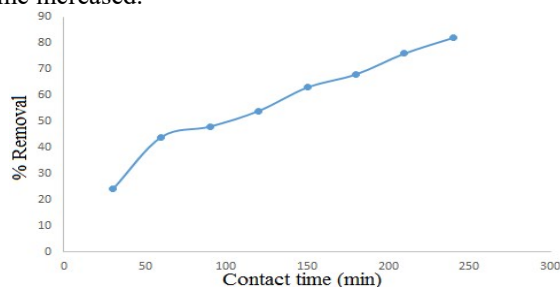


Figure (4) Increasing of MO removal percentage as the contact time increased

Effect of methyl orange concentration: Figure (5) shows the effect of changing the initial concentration of MO in the range of 2.5 to 20 ppm. In the beginning, the adsorption rate improved with the increase of MO concentration. Thus, the maximum MO removal was 64% at a concentration of 10 ppm. Then the removal percentage decreased with increasing MO concentration until it reached 36% when a solution of MO at a concentration of 20 ppm was used. This decrease in removal percentage is due to the saturation of pores available on the surface of the adsorbent (Ruihua et al., 2017).

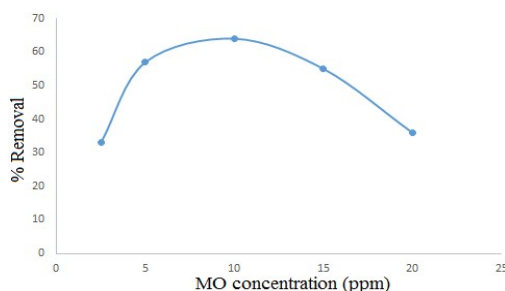


Figure (5) Effect of MO concentration on its removal percentage

Temperature effect: A plot of the removal percentage of MO with initial concentration of 10 ppm at different temperatures (10, 20, 30, and 60 °C) is shown in Fig 6. Generally, the results revealed that the removal percentage increased with increasing temperature for the same MO concentration. The increase in temperature provides a faster rate of diffusion of adsorbate molecules from the solution to the adsorbent. Moreover, increasing the temperature of the solution led to an enlargement of the pore size of OP particles which reduced the resistance of dye molecules to move into OP. As a result of that, the process of MO adsorption on the OP has an endothermic nature.

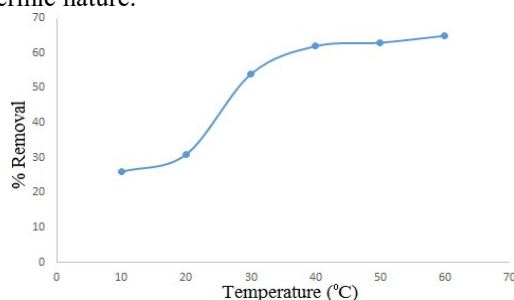


Figure (6) Increasing of MO removal percentage as temperature increased

The effect of agitation speed: In adsorption phenomena, the agitation speed is a significant variable which plays a major role in the distribution of the solute in aqueous solution and the formation of the external boundary film. As can be seen in figure 7, the effect of agitation speed on the removal percentage of MO by OP was investigated at different agitation speeds (0-250 rpm). When the agitation speed increased from 0 to 150 rpm, the removal percentage of MO was observed to rise sharply from 33% to 75% then gradually to 79%. In contrast, the MO adsorption rate decreased from 75% to 70% when the agitation speed exceeded 150 rpm. This decrease could be resulted from desorption of MO as the agitation speed increased.

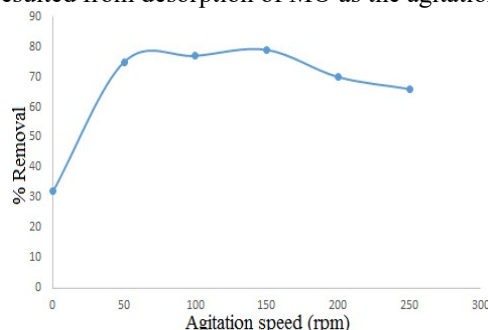


Figure (7) Effect of agitation speed on MO removal percentage



Adsorption kinetic study: The results obtained from the kinetic studies were used in the application of two kinetic models: the pseudo first order model and pseudo second order model. Fig. 8 shows plots of the two kinetic models of MO adsorption onto OP. A comparison of the results with the correlation coefficients is shown in Table 2. The low R^2 value and the difference between experimental q_e and calculated q_e value, obtained by the pseudo-first-order model, indicated that the pseudo-first-order model was not well suited to describe the adsorption of MO by OP. On the other hand, the R^2 value (0.9994) for the pseudo-second-order model was relatively higher than that of the pseudo-first-order model (Table 2). Moreover, the calculated q_e obtained by the pseudo-second-order model was closer to the experimental q_e value. Thus, these results suggest that the pseudo-second-order model provides a good correlation for the MO adsorption process onto OP and that leads to the conclusion that pseudo-second-order model is the best kinetic model that fits MO adsorption behavior.

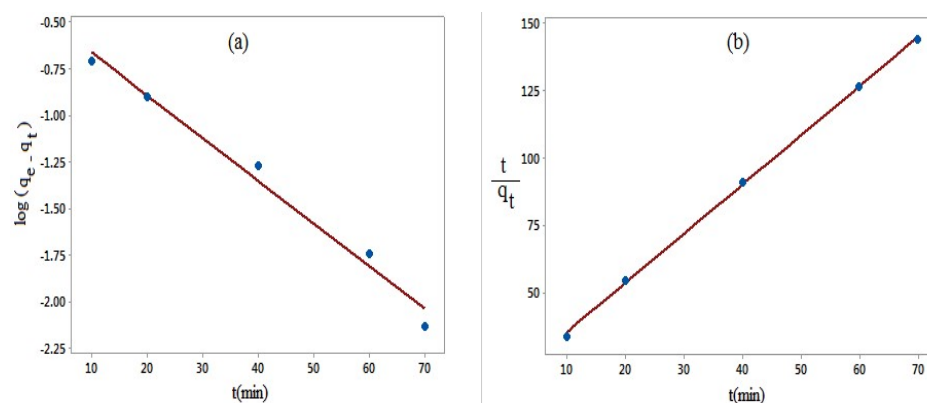


Figure (8) Plots of kinetic models of MO adsorption onto OP: pseudo first-order reaction (a), pseudo second-order reaction (b)

Table 2: Kinetic parameters for adsorption of MO on OP.

q_e (mg/g)	Pseudo first order model			Pseudo second order model		
	q_e (mg/g) Calc.	R^2	K_1 (min^{-1})	q_e (mg/g) calculated	R^2	K_2 ($\text{min}^{-1} \cdot \text{g} \cdot \text{mg}^{-1}$)
Exper. 0.4921	0.3655	0.9849	0.0527	0.5457	0.9994	0.2003

Adsorption isotherm: The obtained results were applied on two equilibrium isotherms, which were the Langmuir and the Freundlich isotherm. Figure 10 shows the relationship plot of Freundlich (Fig 10a) and Langmuir (Fig 10b) models. Using the isotherm data, the coefficient of determination R^2 for both models were calculated, and the results are shown in Table 3. By observing the values of R^2 for both models as shown in Table 3, it is clear that the value of R^2 for the Freundlich model is greater than the R^2 value of the Langmuir model, thus identified as the

better model for the description of MO adsorption isotherm. Since Freundlich model was in a better linearity than Langmuir model, thus the adsorption of MO on OP surface is multilayer (Rattanapan et al., 2017). Because Freundlich model was proved to be the better model its constants (K_f) and (n) were calculated and their values are shown in Table 3, while Langmuir's constants were not calculated as this model did not fit. Since $1/n$ is higher than 1 this indicates that the adsorption process of MO onto OP is cooperative adsorption.

Table 3 Isotherm parameters for adsorption of MO on OP

Langmuir	Freundlich		
R^2	$1/n$	K_f	R^2
0.0049	1.0858	0.0419	0.9183

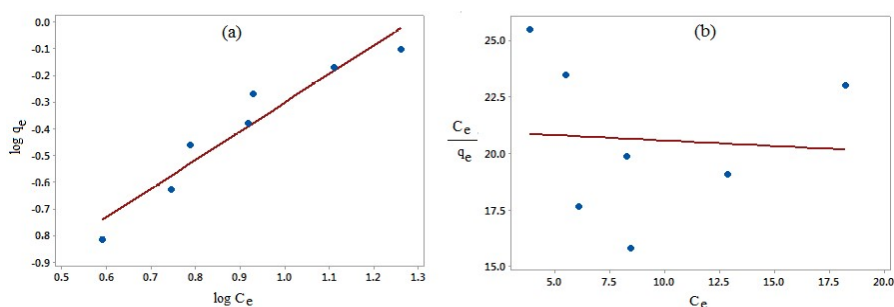


Figure 10: Plots of isotherm models of MO adsorption onto OP: Freundlich isotherm (a), Langmuir isotherm (b)

Conclusion

This study highlighted the possibility of using the OP as an adsorbent of MO from aqueous solutions by applying a simple, inexpensive method. The results showed high adsorption efficiency of olive pomace to remove MO by controlling the factors affecting the adsorption process. The kinetic study of methyl orange adsorption showed that the adsorption follows the pseudo-second order equation and that the time needed to reach the equilibrium state was estimated to be 80 min. The Freundlich model is most suitable for describing isotherm adsorption, which indicates that adsorption occurs in several layers on the surface of the adsorbent. Other studies are needed to investigate the capability of olive pomace to remove other dyes from aqueous solutions.

References

- [1] Li, Y; Sui, K; Liu, R; Zhao, X; Zhang, Y; Liang, H; and Xia, Y. (2012) Removal of methyl orange from aqueous solution by calcium alginate/multi-walled carbon nanotubes composite fibers, *Energy Procedia*, 16 : 863- 868.
- [2] Shashikala, M; Nagapadma, M; Vishnu, P; and Gohain, K. (2014) Adsorption studies on the removal of methylorange dye from aqueous solution using chitosan powder. *JEST-M*, 3: 20-25.



- [3] Anbia, M; and Salehi, S. (2014) Adsorption of methyl orange from aqueous solution onto nanoporous silica materials. *Scientia Iranica C*, 21(6): 2036-2048.
- [4] Saxena, R; and Sharma, S. (2016) Adsorption and kinetic studies on the removal of methyl red from aqueous solutions using low-cost adsorbent: Guar gum powder. *International Journal of Scientific & Engineering Research*, 7:675-683.
- [5] Ismail, B; Hussain, S. T; and Akram, S. (2013) Adsorption of methylene blue onto spinel magnesium aluminate nanoparticles: Adsorption isotherms, kinetic and thermodynamic studies. *Chemical Engineering Journal*, 219: 395–402.
- [6] Sharifi-Yazdi, M. K; Azimi, C; and Khalili, M. B. (2001) Study of the biological treatment of industrial waste water by the activated sludge unit. *Iranian J. Publ. Health*, 30(4): 87-90.
- [7] Eletta, O. A. A; Mustapha, S. I; Ajayi, O. A; and Ahmed, A. T. (2018) Optimization of dye removal from textile wastewater using activated carbon from sawdust, *Nigerian Journal of Technological Development*, 15(1): 26-32.
- [8] Huang, R; Liu, Q; Huo, J; and Yang, B. (2017) Adsorption of methyl orange onto protonated cross-linked chitosan. *Arabian Journal of Chemistry*, 10: 24–32.
- [9] Hassan, A. A; and Abdulhussein, H. A. (2015) Methyl red dye removal from aqueous solution by adsorption on rice hulls. *Journal of Babylon University/Engineering Sciences*, 23(2): pp XX-XX.
- [10] Rattanapan, S; Srikram, J; and Kongsune, P. (2017) Adsorption of methyl orange on coffee grounds activated carbon. *Energy Procedia*, 138: 949-954.
- [11] Patil, S; Renukdas, S; and Patel, N. (2011) Removal of methylene blue, a basic dye from aqueous solutions by adsorption using teak tree (*Tectona grandis*) bark powder. *International Journal of Environmental Sciences*, 1(5): 711-726.
- [12] Alzaydien, A. S. (2015) Adsorption behavior of methyl orange onto wheat bran: Role of surface and pH. *Oriental Journal of Chemistry*, 31(2): 643-651.
- [13] Subbaiah, M; and Su Kim, D. (2016) Adsorption of methyl orange from aqueous solution by aminated pumpkin seed powder: Kinetics, isotherms, and thermodynamic studies. *Ecotoxicology and Environmental Safety*, 128: 109–117.
- [14] Mroweh, A; Hijazi, A; Rammal, H; Alameh, M; Toufaily, J; and Hamieh, T. (2015) Adsorption of Aqueous methyl orange by Lebanese *Eryngium creticum*, *Am.J. Pharm Tech Res*, 5(2):324 -331.
- [15] Sejie, F. P; and Nadiye-Tabbiruka, M. S. (2016) Removal of methyl orange (MO) from water by adsorption onto modified local clay (Kaolinite). *Physical Chemistry*, 6(2): 39-48.
- [16] Vijayakumar, G; Tamilarasan, R; and Dharmendirakumar, M. (2012) Adsorption, kinetic, equilibrium and thermodynamic studies on the removal of basic dye Rhodamine-B from aqueous solution by the use of natural adsorbent perlite. *J. Mater. Environ. Sci*, 3(1): 157-170.
- [17] Allouche, F; Yassaa, N; and Lounici, H. (2015) Sorption of methyl orange from aqueous solution on chitosan biomass. *Procedia Earth and Planetary Science*, 15: 596 – 601.
- [18] Saha, T. K; Bhoumik, N. C; Karmaker, S; Ahmed, M. G; Ichikawa, H; and Fukumori, Y. (2010) Adsorption of methyl orange onto chitosan from aqueous solution. *J. Water Resource and Protection*, 2: 898-906.
- [19] Zouaoui, E; Krid, F; Hermouch, Y; and Medjram, M. S. (2016) Kinetic and thermodynamic study on the removal of methyl orange from aqueous solution by adsorption into pine cone. *Journal of Chemical and Pharmaceutical Sciences*, 9: 39-45
- [20] Al-Ma'amar, A. A. (2012) Sorption study of methyl orange on the Iraqi kaolinite clay. *Journal of Al-Nahrain University Science*, 15(4):98-103.
- [21] Mekatel, E; Amokrane, S; Aid, A; Nibou, D; and Trari, M. (2015) Adsorption of methyl orange on nanoparticles of a synthetic zeolite NaA/CuO, *Comptes Rendus Chimie*, 18: 336–344.
- [22] Bellifa, A; Makhlouf, M; and Boumila, Z. H. (2017) Comparative study of the adsorption of methyl orange by bentonite and activated carbon. *International Conference on Computational and Experimental Science and Engineering (ICCESEN)*, 132(3): 466-468.

- [23] Mouni, L; Belkhiri, L; Bollinger, J; Bouzaza, A; Assadi, A; Tirri, A; Dahmoune, F; Madani, K; and Remini, H. (2018) Removal of methylene blue from aqueous solutions by adsorption on Kaolin: Kinetic and equilibrium studies. *Applied Clay Science*, 153 : 38–45.
- [24] Dim, P. E. (2013) Adsorption of methyl red and methyl orange using different tree bark powder. *Academic Research International*, 4(1): 330-338.
- [25] Hazzaa, R; and Hussein, M. (2015) Cationic dye removal by sugarcane bagasse activated carbon from aqueous solution. *Global Nest Journal*, 17, pp XX-XX.
- [26] Abu -El-Sha'r, W. Y; Gharabieh, S. H; and Mohmoud, S. (1999) Removal of dyes from aqueous solution using low-cost sorbents made of solid residues from olive-mill wastes (JEFT) and solid residues from refined Jordanian oil shale. *Environmental Geology*, 39(10): 1090-1094
- [27] Yagub, M. T; Sen, T. K; Afroze, S; and Ang, H. M. (2014) Dye and its removal from aqueous solution by adsorption: a review. *Advances in colloid and interface science*, 209: 172-184.
- [28] Ahmad, M. A; Puad, N. A; and Bello, O.S. (2014) Kinetic, equilibrium and thermodynamic studies of synthetic dye removal using pomegranate peel activated carbon prepared by microwave-induced KOH activation. *Water Resources and Industry*, 6: 18-35.
- [29] Foo, K. Y; and Hameed, B. H. (2010) Insights into the modeling of adsorption isotherm systems. *Chemical engineering journal*, 156(1): 2-10.
- [30] Sartape, A. S; Mandhare, A. M; Jadhav, V. V; Raut, P. D; Anuse, M. A; and Kolekar, S. S. (2017) Removal of malachite green dye from aqueous solution with adsorption technique using *Limonium acidissimum* (wood apple) shell as low cost adsorbent. *Arabian Journal of Chemistry*, 10: 3229-3238.
- [31] Abd El-Latif, M. A; Ibrahim, A. M; and El-Kady, M. F. (2010) Adsorption equilibrium, kinetics and thermodynamics of methylene blue from aqueous solutions using biopolymer oak sawdust composite. *Journal of American science*, 6(6):267-283.
- [32] Shabudeen, S. P. S. (2011) Adopting response surface methodology to design an experiment in studying the removal of dye by utilizing solid agricultural waste activated carbon. *International Journal of Science and Advanced Technology*, 1(6): 118-127.
- [33] El-Adawy H. A. (2015) Thermodynamics and Adsorption Study of Methyl Orange onto Fired Bricks. *International Journal of Science and Research (IJSR)*, 5: 307-313.
- [34] Jalil, A. A; Triwahyono, S; Adam, S. H; Rahim, N.D; Aziz, M. A; Hairom, N. H; Razali, N. A; Abidin, M. A; Mohamadiah, M. A. (2010) Adsorption of methyl orange from aqueous solution onto calcined Lapindo volcanic mud. *Journal of Hazardous Materials*, 181: 755-762.
- [35] Albroomi, H. I.; Elsayed, M. A.; Baraka, A; and Abdelmaged, M. K. (2015) Factors affecting the removal of a basic and an azo dye from artificial solutions by adsorption using activated carbon. *Journal of the Turkish Chemical Society, Section A: Chemistry*, 2: 17-33